

---

## CHAPTER 3

# HAMILTON'S EQUATIONS WITH EULER PARAMETERS FOR RIGID BODY DYNAMICS MODELING

Ravishankar Shivarama<sup>1</sup> and Eric P. Fahrenthold<sup>2</sup>

Department of Mechanical Engineering, 1 University Station C2200  
University of Texas, Austin, TX 78712, USA

---

<sup>1</sup>Graduate student

<sup>2</sup>Professor, corresponding author, phone: (512) 471-3064, email: epfahren@mail.utexas.edu

# HAMILTON'S EQUATIONS WITH EULER PARAMETERS FOR RIGID BODY DYNAMICS MODELING

Ravishankar Shivarama<sup>3</sup> and Eric P. Fahrenthold<sup>4</sup>

Department of Mechanical Engineering, University of Texas, Austin, TX 78712

*A combination of Euler parameter kinematics and Hamiltonian mechanics provides a rigid body dynamics model well suited for use in strongly nonlinear problems involving arbitrarily large rotations. The model is unconstrained, free of singularities, includes a general potential energy function and a minimum set of momentum variables, and takes an explicit state space form convenient for numerical implementation. The general formulation may be specialized to address particular applications, as illustrated in several three dimensional example problems.*

## INTRODUCTION

A variety of rigid body dynamics modeling problems demand consideration of very large rotations. Some of the best known examples involve aircraft [1] and spacecraft [2,16], although the analysis of large rotation dynamics is of generic interest in a wide range of applications, including mechanism and machine theory [3,4] and molecular dynamics [12]. Most models of rigid body dynamics problems employ Euler angles [5]. Such formulations lead to equations of motion which are unconstrained, but which contain singularities [1]. Other singular three parameter methods have been developed, including for example those of Laning-Bortz-Stuelpnagel [11] and Rodriguez [13]. The presence of singularities in all these methods has motivated the development of alternative four parameter modeling schemes [11], including Euler parameters [15]. Such formulations replace the three Euler angles with four

---

<sup>3</sup>Graduate research assistant

<sup>4</sup>Professor

parameters and an algebraic constraint. This avoids the Euler angle singularities but leads nominally to a system level model in differential-algebraic form.

In an attempt to avoid both singular equations of motion and differential-algebraic systems, several authors have presented reformulations of Euler parameter based models, for use in three dimensional rigid body dynamics problems. Chang et al. [2], Nikravesh and co-workers [7,8,9,10], and Vadali [17] present alternative formulations based on Lagrange's equations. Since Lagrange's method defines the solution as a path in configuration space, and since the Euler parameters are taken as generalized coordinates, this approach starts with a differential system of order eight (four second order equations for the rotational dynamics of a single rigid body) augmented with a single algebraic constraint. Nikravesh and co-workers begin from this starting point and proceed to find a closed form solution for the Lagrange multiplier associated with the algebraic constraint, resulting in an unconstrained formulation of order eight. They do not include a potential energy function in the system Lagrangian. Similar results are obtained by Vadali. Proceeding in a different manner, Chang et al. introduce as quasi-velocity variables the rigid body angular velocities in the body fixed frame, and project the original order eight Lagrange equations onto an order seven subspace. In the process they eliminate the unknown Lagrange multiplier.

As an alternative to Lagrange's equations, a Hamiltonian formulation of rigid body dynamics with Euler parameters has been proposed by Morton [6]. However his final formulation is of order eight, and includes a superfluous momentum variable as well as a 'generally arbitrary' unspecified scalar parameter. It appears that no previous work has attempted to revise or improve upon the Morton formulation.

The usefulness of formulations based on Hamilton's canonical equations is well recognized [3]. They offer an explicit state space description of system dynamics problems which is: (a) convenient for numerical integration, (b) well suited for coupling to automatic control system models, and (c) energy based and hence providing clear physical insight. Recognizing these strengths, a revision and extension of existing Hamiltonian formulations for rigid body

dynamics is of generic interest. The present paper presents such work, deriving unconstrained Hamilton's equations for the three dimensional dynamics of a rigid body in terms of Euler parameters, and hence suitable for use in simulations involving arbitrary rotational motion. The derivation avoids any requirement to determine the Lagrange multiplier associated with the Euler parameter constraint. No arbitrary parameters are introduced, and the final rotational formulation is of order seven. A general potential energy function and nonpotential virtual work effects are included in the model. Validation and application of the method is illustrated here in several three dimensional example problems.

## KINEMATICS

This section defines the kinematic variables of interest, and recalls a number of well known kinematic relations [1], for use in succeeding sections.

The position and orientation of an arbitrary rigid body is described here in terms of seven generalized coordinates, namely the Cartesian components of the center of mass vector ( $\mathbf{c}$ ) and a four component vector of Euler parameters ( $\mathbf{e}$ )

$$\mathbf{c} = [c_1 \ c_2 \ c_3]^T, \quad \mathbf{e} = [e_0 \ e_1 \ e_2 \ e_3]^T \quad (1)$$

Knowledge of the Euler parameters determines a (nonunique) set of Euler angles ( $\phi, \theta, \psi$ ) for the body, associated with a 3-1-3 rotation sequence, via the relations

$$\phi = \tan^{-1}\left(\frac{e_3}{e_0}\right) + \tan^{-1}\left(\frac{e_2}{e_1}\right) \quad (2)$$

$$\psi = \tan^{-1}\left(\frac{e_3}{e_0}\right) - \tan^{-1}\left(\frac{e_2}{e_1}\right) \quad (3)$$

$$\theta = 2 \sin^{-1}\left(\sqrt{e_1^2 + e_2^2}\right) \quad (4)$$

The Euler parameters define an orthogonal rotation matrix ( $\mathbf{R}$ ) which relates the vector of components ( $\mathbf{a}$ ) of a first order tensor described in a fixed Cartesian coordinate system to a corresponding vector of components ( $\hat{\mathbf{a}}$ ) described in a body fixed co-rotating frame, using

$$\mathbf{a} = \mathbf{R} \hat{\mathbf{a}} \quad (5)$$

where

$$\mathbf{R} = \mathbf{E} \mathbf{G}^T \quad (6)$$

with

$$\mathbf{E} = \begin{bmatrix} -e_1 & e_0 & -e_3 & e_2 \\ -e_2 & e_3 & e_0 & -e_1 \\ -e_3 & e_2 & e_1 & e_0 \end{bmatrix} \quad (7)$$

$$\mathbf{G} = \begin{bmatrix} -e_1 & e_0 & e_3 & -e_2 \\ -e_2 & -e_3 & e_0 & e_1 \\ -e_3 & -e_2 & -e_1 & e_0 \end{bmatrix} \quad (8)$$

The four Euler parameters are not independent, and satisfy the constraint equation

$$\mathbf{e}^T \mathbf{e} = 1 \quad (9)$$

which then implies

$$\mathbf{G} \mathbf{G}^T = \mathbf{I} \quad (10)$$

where  $\mathbf{I}$  is an order three identity matrix. In addition,  $\mathbf{G}$  and  $\mathbf{e}$  and their time derivatives satisfy the identities

$$\mathbf{G} \mathbf{e} = \mathbf{0}, \quad \mathbf{G} \dot{\mathbf{e}} = -\dot{\mathbf{G}} \mathbf{e} \quad (11)$$

The kinematic equations [1] which relate the time derivatives of the Euler parameters to the components of the angular velocity vector ( $\boldsymbol{\omega}$ ) of the rigid body, expressed in the body-fixed co-rotating frame, are

$$\boldsymbol{\omega} = 2 \mathbf{G} \dot{\mathbf{e}}, \quad \dot{\mathbf{e}} = \frac{1}{2} \mathbf{G}^T \boldsymbol{\omega} \quad (12)$$

Finally note that the skew-symmetric matrix  $\boldsymbol{\Omega}$ , with axial vector  $\boldsymbol{\omega}$ , which satisfies

$$\boldsymbol{\Omega} \mathbf{v} = \boldsymbol{\omega} \times \mathbf{v} \quad (13)$$

for any vector  $\mathbf{v}$ , is related to the Euler parameters and their time derivatives by

$$\boldsymbol{\Omega} = 2 \mathbf{G} \dot{\mathbf{G}}^T = -2 \dot{\mathbf{G}} \mathbf{G}^T \quad (14)$$

The next section defines kinetic and potential energy functions and hence the Hamiltonian for the system of interest.

## KINETIC AND POTENTIAL ENERGY

The complementary kinetic energy for the rigid body may be expressed as

$$T^* = \frac{1}{2} m \dot{\mathbf{c}}^T \dot{\mathbf{c}} + \frac{1}{2} \boldsymbol{\omega}^T \mathbf{J} \boldsymbol{\omega} \quad (15)$$

where  $m$  is the mass and  $\mathbf{J}$  is a constant matrix of components for the moment of inertia tensor of the body, referred to the co-rotating frame. In terms of the Euler parameters and their time derivatives,

$$T^* = \frac{1}{2} m \dot{\mathbf{c}}^T \dot{\mathbf{c}} + 2 \dot{\mathbf{e}}^T \mathbf{G}^T \mathbf{J} \mathbf{G} \dot{\mathbf{e}} \quad (16)$$

which has the form  $T^* = T^*(\dot{\mathbf{c}}, \dot{\mathbf{e}}, \mathbf{e})$ . It follows that the generalized momenta are

$$\mathbf{p} = \frac{\partial T^*}{\partial \dot{\mathbf{c}}} = m \dot{\mathbf{c}}, \quad \mathbf{g} = \frac{\partial T^*}{\partial \dot{\mathbf{e}}} = 4 \mathbf{G}^T \mathbf{J} \mathbf{G} \dot{\mathbf{e}} \quad (17)$$

Note that the identities (10) through (12) require

$$\mathbf{g} = 2 \mathbf{G}^T \mathbf{J} \boldsymbol{\omega}, \quad \boldsymbol{\omega} = \frac{1}{2} \mathbf{J}^{-1} \mathbf{G} \mathbf{g} \quad (18)$$

Since the complimentary rotational kinetic energy may also be expressed, using equation (11), as

$$T_{rot}^* = 2 \mathbf{e}^T \dot{\mathbf{G}}^T \mathbf{J} \dot{\mathbf{G}} \mathbf{e} \quad (19)$$

then the Euler parameter dependence of  $T^*$  defines the partial derivative

$$\mathbf{k} = \frac{\partial T^*}{\partial \mathbf{e}} = 4 \dot{\mathbf{G}}^T \mathbf{J} \dot{\mathbf{G}} \mathbf{e} \quad (20)$$

The kinetic energy of the body is defined via the Legendre transform

$$T = \mathbf{p}^T \dot{\mathbf{c}} + \mathbf{g}^T \dot{\mathbf{e}} - T^* \quad (21)$$

so that the preceding results lead to the canonical form  $T = T(\mathbf{p}, \mathbf{g}, \mathbf{e})$  which is

$$T = \frac{1}{2} m^{-1} \mathbf{p}^T \mathbf{p} + \frac{1}{8} \mathbf{g}^T \mathbf{G}^T \mathbf{J}^{-T} \mathbf{G} \mathbf{g} \quad (22)$$

and require that (see the appendix)

$$-\mathbf{k} = \frac{\partial T}{\partial \mathbf{e}} \quad (23)$$

For the mechanical systems considered here, the potential energy function has the general form

$$V = V(\mathbf{c}, \mathbf{e}) \quad (24)$$

and the system Hamiltonian is

$$H = T + V \quad (25)$$

The next section introduces a virtual work expression, to account for nonpotential effects.

## NONPOTENTIAL VIRTUAL WORK

The quasi-coordinates  $\mathbf{q}$  associated with the co-rotating components of the angular velocity vector are defined by

$$\dot{\mathbf{q}} = \boldsymbol{\omega} \quad (26)$$

In terms of the latter coordinates, and the center of mass coordinates, the nonpotential virtual work due to the imposed forces  $\mathbf{f}(t)$  and torques  $\mathbf{T}(t)$  is

$$\delta W_{nc} = \mathbf{f}(t)^T \delta \mathbf{c} + \mathbf{T}(t)^T \delta \mathbf{q} \quad (27)$$

Since

$$\delta \mathbf{q} = 2 \mathbf{G} \delta \mathbf{e} \quad (28)$$

the virtual work expression which defines the generalized nonpotential forces is

$$\delta W_{nc} = \mathbf{f}(t)^T \delta \mathbf{c} + 2 [\mathbf{G}^T \mathbf{T}(t)]^T \delta \mathbf{e} \quad (29)$$

Note that damping effects may contribute additional terms to the nonpotential virtual work, in which case the nonpotential forces may depend on the generalized coordinates and velocities. In addition the presence of nonholonomic constraints may introduce terms which depend on unknown Lagrange multipliers. The last problem discussed in the examples section illustrates the effects of both damping and nonholonomic constraints.

The next section derives Hamilton's equations for the system.

## HAMILTON'S EQUATIONS

The system Hamiltonian has the form  $H = H(\mathbf{p}, \mathbf{c}, \mathbf{g}, \mathbf{e})$  and the canonical Hamilton's equations are

$$\dot{\mathbf{p}} = -\frac{\partial H}{\partial \mathbf{c}} + \mathbf{f}^p, \quad \dot{\mathbf{c}} = \frac{\partial H}{\partial \mathbf{p}} \quad (30)$$

and

$$\dot{\mathbf{g}} = -\frac{\partial H}{\partial \mathbf{e}} + \mathbf{f}^g, \quad \dot{\mathbf{e}} = \frac{\partial H}{\partial \mathbf{g}} \quad (31)$$

where  $\mathbf{f}^p$  and  $\mathbf{f}^g$  are the nonpotential generalized forces associated with the virtual work and any applied constraints. The Euler parameter constraint has the rate form

$$\dot{\mathbf{e}}^T \mathbf{e} = 0 \quad (32)$$

Introducing a Lagrange multiplier  $\lambda$ , the latter constraint combines with the virtual work expression to yield

$$\mathbf{f}^p = \mathbf{f}(t) \quad (33)$$

$$\mathbf{f}^g = 2 \mathbf{G}^T \mathbf{T}(t) + \lambda \mathbf{e} \quad (34)$$

so that for the derived Hamiltonian the momentum balance equations are

$$\dot{\mathbf{p}} = -\frac{\partial V}{\partial \mathbf{c}} + \mathbf{f}(t) \quad (35)$$

$$\dot{\mathbf{g}} = -\frac{\partial V}{\partial \mathbf{e}} + \mathbf{k} + 2 \mathbf{G}^T \mathbf{T}(t) + \lambda \mathbf{e} \quad (36)$$

The last equation includes an unknown Lagrange multiplier and a superfluous momentum variable. These variables are eliminated by introducing the three-momentum vector

$$\mathbf{h} = \mathbf{J} \boldsymbol{\omega} \quad (37)$$

whose time derivative is

$$\dot{\mathbf{h}} = \frac{1}{2} \mathbf{G} \dot{\mathbf{g}} + \frac{1}{2} \dot{\mathbf{G}} \mathbf{g} \quad (38)$$



With equations (11) and (36) this yields

$$\dot{\mathbf{h}} = \frac{1}{2}\dot{\mathbf{G}}\mathbf{g} + \frac{1}{2}\mathbf{G}\mathbf{k} + \mathbf{T}(t) - \frac{1}{2}\mathbf{G}\frac{\partial V}{\partial \mathbf{e}} \quad (39)$$

or

$$\dot{\mathbf{h}} = -\frac{1}{2}\boldsymbol{\Omega}\mathbf{h} + \frac{1}{2}\mathbf{G}\mathbf{k} + \mathbf{T}(t) - \frac{1}{2}\mathbf{G}\frac{\partial V}{\partial \mathbf{e}} \quad (40)$$

which eliminates both  $\lambda$  and the four component momentum vector.

The final unconstrained Hamiltonian model is

$$\dot{\mathbf{p}} = -\frac{\partial V}{\partial \mathbf{c}} + \mathbf{f}(t) \quad (41)$$

$$\dot{\mathbf{h}} = -\boldsymbol{\Omega}\mathbf{h} - \frac{1}{2}\mathbf{G}\frac{\partial V}{\partial \mathbf{e}} + \mathbf{T}(t) \quad (42)$$

$$\dot{\mathbf{c}} = m^{-1}\mathbf{p} \quad (43)$$

$$\dot{\mathbf{e}} = \frac{1}{2}\mathbf{G}^T\mathbf{J}^{-1}\mathbf{h} \quad (44)$$

Given a potential function and the virtual work, the preceding explicit equations may be integrated to simulate the system response.

As outlined in the introduction, the rigid body dynamics formulation derived here combines the advantages of Hamiltonian mechanics and Euler parameter kinematics. Hamiltonian and Lagrangian methods generally simplify the model formulation process, in particular when geometric nonlinearities are important. Such nonlinearities arise for example when large rotations or hyperelastic devices are of interest. As compared to Lagrangian methods, Hamiltonian methods offer an explicit state space description of the system dynamics, normally most convenient for numerical integration. Euler parameters offer a singularity free description of rotational displacements, and are therefore preferred over Euler angle models in large rotation applications. The cost is of course the need to integrate an additional state equation for each rigid body, since the Euler parameters are a quaternion. The present combination of Hamiltonian mechanics and Euler parameter kinematics is therefore of most interest in the formulation and numerical integration of models for strongly nonlinear mechanical systems. The model developed here is unique in its combination of features:

unconstrained, free of singularities, incorporating a general potential energy function, employing a minimum set of momentum variables, and taking an explicit state space form convenient for numerical implementation.

## EXAMPLE PROBLEMS

Application of the Hamiltonian formulation developed here is illustrated in four examples. The first example compares an Euler angle based model of a rotating disk problem to the present Hamiltonian formulation, both to validate the present approach and to illustrate in a simple case an Euler parameter description of rotational displacement. The second example solves a classical rigid body dynamics problem for the three dimensional motion of a torque-free body, for comparison to the published numerical solution of Morton [6] and to the partial analytical solution of Thompson [16]. This problem again validates the present approach, and compares a discontinuous Euler angle description of three dimensional rigid body motion to the continuous Euler parameter characterization adopted here. The third example models a spinning top in a uniform gravitational field, a problem described in many advanced dynamics tests, and validates the present formulation in a three dimensional rigid body motion involving both translation and rotation. Here a numerical solution for the last cited problem is obtained using a time step identical to that employed by Simo and Wong [14], but without resort to their symplectic integration algorithm. The last example considers a problem of practical importance in the design of gyroscopic seekers, namely the motion of a freely precessing body with a viscous ring nutation damper [2]. This example calls for the application of nonholonomic constraints. Here we develop an explicit state space model, as compared to the implicit Lagrangian formulation [2] of Chang et al.

The first example models the free vibration of a rigid circular disk of radius  $r$ , rotating about a fixed point, and attached to a linear spring of stiffness  $k$  (see Figure 1). The potential energy function is

$$V = \frac{1}{2} k y_p^2 = \frac{1}{2} k r^2 [2e_1e_2 + 2e_0e_3]^2 \quad (45)$$

where  $y_p$  denotes the vertical displacement of the point of attachment of the spring, measured in a Cartesian coordinate system whose origin lies at the center of the disk. Note that the indicated Euler parameter dependence of the potential energy is obtained using equation (5). Assuming the model parameters and initial conditions listed in Table 1, the motion was simulated by integration of a Newtonian model based on the Euler angle  $\phi$

$$J\ddot{\phi} + \frac{1}{2} k r \sin(2\phi) = 0 \quad (46)$$

and by integration of the Hamiltonian relations (42) and (44). The two computed results for the angular momentum are compared in Figure 2, showing excellent agreement of the Euler angle based and Euler parameter based solutions. Figure 3 shows the computed variation of the Euler parameters with time.

The second example models the torque free motion of a rigid body, for the inertial properties and initial conditions listed in Table 2. A partial analytical solution for this classic problem is known and can be expressed in terms of elliptic functions [6,16]. Figures 4 and 5 shown the time variation of the angular momenta and Euler parameters computed using the present Hamiltonian formulation. Figure 6 plots the implied Euler angles, emphasizing the discontinuous nature of the latter variables. Table 3 shows excellent agreement of the analytical and numerical solutions for the amplitudes and periods of the angular momenta, in three dimensional motion.

The third example models the translational and rotational motion of a spinning top in a uniform gravitational field. This problem is described in many advanced dynamics texts [4], and is used by Simo and Wong [14] to evaluate their symplectic numerical integration scheme. The potential energy for the system is

$$V = W z_c \quad (47)$$

where  $W$  is the weight of the top and  $z_c$  is the vertical coordinate of the center of mass. The simulation parameters and initial conditions for the problem are listed in Table 4. Figures 7

and 8 show numerical results for the normalized angular momentum components and center of mass coordinates, obtained by integration of Hamilton's equations (41) through (44), using a fourth order Runge-Kutta method. Table 5 compares an approximate analytical estimate of the nutation and precession frequencies for the top, provided by Goldstein [4], to the present numerical results. The present numerical results are identical to those plotted by Simo and Wong [14], and are obtained using the same time step, but without resort to their symplectic integration scheme.

The fourth example considers the rotational motion of a rigid rotor damped by a partially filled mercury ring damper. The reader is referred to Chang et al. [2] for a detailed discussion of this problem, and its application in the analysis of gyroscopic seekers. We focus here on the formulation of a dynamic model for the system analyzed in reference [2]. The paragraphs which follow develop an explicit Hamiltonian model for this system, an alternative to the implicit Lagrangian model of Chang et al., adopting their stipulated assumptions on stored energy functions, energy dissipation, and kinematic constraints.

The rotor is modeled as a rigid circular cylinder with a fixed center of mass located at the origin of a global XYZ coordinate system. The partially filled mercury ring damper is a cylinder of mean radius  $R$ , co-axial with and external to the rotor, with a centroid displaced a distance  $L$  along the rotor axis from the rotor center of mass location. Body-fixed coordinate systems for the rotor ( $xyz$ ) and ring ( $uvw$ ) are co-located at the centroid of the damper, where the  $z$  direction is aligned with the rotor axis. The partial mercury ring is free to rotate about the rotor axis, subject to a damping torque which is linear in the axial angular velocity difference between the rotor and the ring, but is otherwise constrained to move with the rotor. Hence the orientations of the body-fixed axes systems which co-rotate with the rotor and the ring differ only by an angle  $\beta$ , which describes the axial rotation of the ring with respect to the rotor.

The assumed complimentary kinetic energy for the system is [2]

$$T^* = \frac{1}{2} \boldsymbol{\omega}^T \mathbf{J}^T \boldsymbol{\omega} + \frac{1}{2} \boldsymbol{\omega}_m^T \mathbf{J}_m^T \boldsymbol{\omega}_m \quad (48)$$

where  $\boldsymbol{\omega}$  and  $\boldsymbol{\omega}_m$  are angular velocities for the rotor and ring and

$$\mathbf{J} = \begin{bmatrix} J_1 & 0 & 0 \\ 0 & J_2 & 0 \\ 0 & 0 & J_3 \end{bmatrix}, \quad \mathbf{J}_m = \begin{bmatrix} J_{m1} & 0 & -J_{m4} \\ 0 & J_{m2} & 0 \\ -J_{m4} & 0 & J_{m3} \end{bmatrix} \quad (49)$$

are constant moment of inertia matrices for the rotor and ring. All four quantities are described in the respective rotor and ring body-fixed co-rotating coordinate systems.

The assumed potential energy for the system, due to the gravitational potential of the mercury, is [2]

$$V = -m \mathbf{g}_c \mathbf{R}^T \mathbf{B}^T \mathbf{r}_c, \quad \mathbf{r}_c = [R \sin(\gamma/2)/(\gamma/2), 0, L]^T \quad (50)$$

where  $m$  is the mass of the mercury,  $\mathbf{g}_c$  is a constant gravity acceleration vector described in the fixed  $XYZ$  frame,  $\mathbf{R}$  is the rotation matrix of equation (6), whose Euler parameters ( $\mathbf{e}$ ) refer to the rotor-fixed frame,  $\mathbf{r}_c$  is a constant vector which locates the mercury center of mass,  $\gamma$  is the angle which subtends the mercury arc (symmetric about the  $u$  axis), and  $\mathbf{B}$  is an orthogonal matrix which defines the transformation of vector components from the rotor-fixed to the ring-fixed frame

$$\mathbf{B} = \begin{bmatrix} \cos(\beta) & \sin(\beta) & 0 \\ -\sin(\beta) & \cos(\beta) & 0 \\ 0 & 0 & 1 \end{bmatrix} \quad (51)$$

Note that  $V = V(\mathbf{e}, \beta)$ . The virtual work for the system, due to damping at the ring-rotor interface, is [2]

$$\delta W = -C_d R^2 \dot{\beta} \delta\beta \quad (52)$$

where  $C_d$  is an empirical dimensionless damping coefficient.

Given the preceding modeling assumptions, Hamilton's equations for the rotor and ring

system are

$$\dot{\mathbf{h}} = -\boldsymbol{\Omega}\mathbf{h} - \frac{1}{2}\mathbf{G}\frac{\partial V}{\partial \mathbf{e}} + \mathbf{T} \quad (53)$$

$$\dot{\mathbf{h}}_m = -\boldsymbol{\Omega}_m\mathbf{h}_m + \mathbf{T}_m \quad (54)$$

$$\dot{\mathbf{e}} = \frac{1}{2}\mathbf{G}^T\mathbf{J}^{-1}\mathbf{h} \quad (55)$$

$$0 = -\frac{\partial V}{\partial \beta} + T_\beta \quad (56)$$

where  $\mathbf{h}$  and  $\mathbf{h}_m$  are angular momenta for the rotor and ring

$$\mathbf{h} = \mathbf{J}\boldsymbol{\omega}, \quad \mathbf{h}_m = \mathbf{J}_m\boldsymbol{\omega}_m \quad (57)$$

and  $\mathbf{T}$ ,  $\mathbf{T}_m$ , and  $T_\beta$  are nonpotential forces due to damping and kinematic constraints. Note that the degenerate form of Hamilton's equation for  $\beta$  is due to the fact that the latter generalized coordinate, which appears in the potential energy function, is not associated with a corresponding generalized momentum variable. The kinematic constraints are [2]

$$\omega_{m1} = \cos(\beta)\omega_1 + \sin(\beta)\omega_2, \quad \omega_{m2} = -\sin(\beta)\omega_1 + \cos(\beta)\omega_2, \quad (58)$$

and

$$\dot{\beta} = \omega_{m3} - \omega_3 \quad (59)$$

They quantify the aforementioned modeling assumption that the ring moves relative to the rotor only in axial rotation.

An explicit state space model may be obtained by application of the constraints, as follows. Introducing a Lagrange multiplier  $\mu$  for the constraint (59), and accounting for the virtual work, requires

$$T_\beta = \mu - C_d R^2 \dot{\beta}, \quad \mathbf{T} = \mu \mathbf{c}, \quad \mathbf{T}_m = -\mu \mathbf{c} \quad (60)$$

where  $\mathbf{c}$  denotes the vector  $[0, 0, 1]^T$ . The degenerate Hamilton's equation for  $\beta$  therefore determines the Lagrange multiplier as

$$\mu = C_d R^2 \dot{\beta} + \frac{\partial V}{\partial \beta} \quad (61)$$

Hamilton's equation (54) for the ring angular momentum may now be written in the form

$$\dot{\boldsymbol{\omega}}_m = -\mathbf{J}_m^{-1}\boldsymbol{\Omega}_m\mathbf{J}_m\boldsymbol{\omega}_m - \mu\mathbf{J}_m^{-1}\mathbf{c} \quad (62)$$

Since the constraints specify both  $\dot{\beta}$  and the first two components of the ring angular velocity vector as functions of the set  $(\beta, \omega_1, \omega_2, \omega_{m3})$ , the third of equations (62) is an evolution relation for the unknown  $\omega_{m3}$ . Combining the third of equations (62) with the constraint equation (59), the constitutive relations (57), and Hamilton's equations (53) and (55), the result is an explicit state space model of order nine for the ring-rotor system. The final state equations are

$$\dot{\mathbf{h}} = -\boldsymbol{\Omega}\mathbf{h} - \frac{1}{2}\mathbf{G}\frac{\partial V}{\partial \mathbf{e}} + \left[ C_d R^2 \left( \omega_{m3} - \frac{h_3}{J_3} \right) + \frac{\partial V}{\partial \beta} \right] \mathbf{c} \quad (63)$$

$$\dot{\mathbf{e}} = \frac{1}{2}\mathbf{G}^T\mathbf{J}^{-1}\mathbf{h} \quad (64)$$

$$\dot{\beta} = \omega_{m3} - \frac{h_3}{J_3} \quad (65)$$

$$\dot{\omega}_{m3} = -\mathbf{c}^T (\mathbf{J}_m^{-1}\boldsymbol{\Omega}_m\mathbf{J}_m\boldsymbol{\omega}_m) - \left[ C_d R^2 \left( \omega_{m3} - \frac{h_3}{J_3} \right) + \frac{\partial V}{\partial \beta} \right] \mathbf{c}^T \mathbf{J}_m^{-1}\mathbf{c} \quad (66)$$

where

$$\boldsymbol{\Omega} = \boldsymbol{\Omega}(\mathbf{h}), \quad \mathbf{G} = \mathbf{G}(\mathbf{e}), \quad \boldsymbol{\Omega}_m = \boldsymbol{\Omega}_m(\boldsymbol{\omega}_m) \quad (67)$$

with

$$\omega_{m1} = \cos(\beta) \frac{h_1}{J_1} + \sin(\beta) \frac{h_2}{J_2}, \quad \omega_{m2} = -\sin(\beta) \frac{h_1}{J_1} + \cos(\beta) \frac{h_2}{J_2} \quad (68)$$

Note that implicit model of reference [2] is also of order nine but employs a different set of state variables.

## CONCLUSION

The present paper has derived and applied a new Hamiltonian formulation of rigid body dynamics problems, based on Euler parameter kinematics. Euler parameter kinematics provide a singularity free description of three dimensional rigid body motion, accommodating arbitrarily large rotations. When combined with Hamiltonian mechanics, the result is an

energy based modeling approach well suited to address problems with complex geometric nonlinearities. As compared to previous work, the formulation derived here offers a unique combination of features. It avoids the introduction of algebraic constraints and unspecified parameters, includes a general potential energy function, incorporates a minimum set of momentum variables, and takes an explicit state space form convenient for use in control related applications.

## **ACKNOWLEDGEMENTS**

This work was supported by NASA Johnson Space Center (NAG9-1244), the National Science Foundation (CMS99-12475), and the State of Texas Advanced Research Program (003658-0709-1999). Computer time support was provided by the NASA Advanced Supercomputing Division (ARC) and the Texas Advanced Computing Center (UTA).



## APPENDIX

A complimentary kinetic energy expression ( $T^*$ ) with the functional form

$$T^* = T^*(\mathbf{e}, \mathbf{f}), \quad \mathbf{f} = \dot{\mathbf{e}} \quad (69)$$

has the total differential

$$dT^* = \mathbf{g}^T d\mathbf{f} + \frac{\partial T^{*T}}{\partial \mathbf{e}} d\mathbf{e}, \quad \mathbf{g} = \frac{\partial T^*}{\partial \mathbf{f}} \quad (70)$$

The corresponding kinetic energy function ( $T$ ) is determined by the Legendre transform

$$T = \mathbf{g}^T \mathbf{f} - T^* \quad (71)$$

and has a total differential defined by

$$dT = \mathbf{g}^T d\mathbf{f} + \mathbf{f}^T d\mathbf{g} - dT^* = \mathbf{f}^T d\mathbf{g} - \frac{\partial T^{*T}}{\partial \mathbf{e}} d\mathbf{e} \quad (72)$$

as well as the canonical form

$$dT = \frac{\partial T^T}{\partial \mathbf{g}} d\mathbf{g} + \frac{\partial T^T}{\partial \mathbf{e}} d\mathbf{e} \quad (73)$$

It follows that

$$\mathbf{f} = \frac{\partial T}{\partial \mathbf{g}}, \quad \frac{\partial T}{\partial \mathbf{e}} = -\frac{\partial T^*}{\partial \mathbf{e}} \quad (74)$$

## REFERENCES

- [1] Baruh, Haim, 1999, ANALYTICAL DYNAMICS, McGraw Hill, New York.
- [2] Chang C.O., Chou, C.S., and Wang, S.Z., 1991, Design of a viscous ring nutation damper for a freely precessing body, *Journal of Guidance, Control and Dynamics*, **14**, pp. 1136-1144.
- [3] Ginsberg, J.H., 1988, ADVANCED ENGINEERING DYNAMICS, Harper and Row, New York.
- [4] Goldstein, Herbert, 1965, CLASSICAL MECHANICS, Addison-Wesley Publishing Company, New York.
- [5] Greenwood, Donald T., 1988, PRINCIPLES OF DYNAMICS, Prentice Hall, Englewood Cliffs, New Jersey.
- [6] Morton, Harold S., Jr., 1993, Hamiltonian and lagrangian formulations of rigid body rotational dynamics based on euler parameters, *The Journal of Astronautical Sciences*, **41**, pp. 561-5991.
- [7] Nikravesh, P.E., and Chung, I.S., 1982, Application of euler parameters to the dynamic analysis of three dimensional constrained mechanical systems, *Journal of Mechanical Design*, **104**, pp. 785-791.
- [8] Nikravesh, P.E., Wehage, R.A., and Kwon, O.K., 1985, Euler parameters in computational kinematics and dynamics: part 1, *Journal of Mechanisms, Transmissions and Automation Design*, **107**, pp. 358-365.
- [9] Nikravesh, P.E., Kwon, O.K., and Wehage, R.A., 1985, Euler parameters in computational kinematics and dynamics: part 2, *Journal of Mechanisms, Transmissions and Automation Design*, **107**, pp. 366-369.
- [10] Nikravesh, P.E., 1988, COMPUTER AIDED ANALYSIS OF MECHANICAL SYSTEMS, Prentice Hall, Englewood Cliffs, New Jersey.
- [11] Nitschke, M., and Knickmeyer, E.H., 2000, Rotation parameters- a survey of techniques, *Journal of Surveying Engineering*, **126**, pp. 83-105.
- [12] Rapaport, D.C., 1985, Molecular dynamics simulation using quaternions, *Journal of Computational Physics*, **41**, pp. 306-314.

- [13] Shuster, M.D., 1993, A survey of attitude representations, *Journal of Astronautical Sciences*, **41**, pp. 531-543.
- [14] Simo, J.C., and Wong, K.K., 1991, Unconditionally stable algorithms for rigid body dynamics that exactly preserve energy and momentum, *International Journal of Numerical methods in Engineering*, **31**, pp. 19-52.
- [15] Spring, K.W., 1986, Euler parameters and the use of quaternion algebra in the manipulation of finite rotations: a review, *Mechanism and Machine Theory*, **21**, pp. 365-373.
- [16] Thompson, W.T., 1961, INTRODUCTION TO SPACE DYNAMICS, John Wiley and Sons, New York.
- [17] Vadali, S.R., 1988, On the euler parameter constraint, *The Journal of Astronautical Sciences*, **36**, pp. 259-265.

Parameter	value
Mass moment of inertia ( $kg\ m^2$ )	$J = 2$
Radius of the disk ( $m$ )	$r = 1$
Stiffness of the spring ( $N/m$ )	$k = 10$
Initial displacement ( <i>degrees</i> )	$\phi = 30$
Initial momentum ( $kg\ m^2rad/s$ )	$h = 0$

Table 1: Model parameters and initial conditions for the first example problem

Parameter	value
Mass moments of inertia ( $kg\ m^2$ )	$J_1 = 400, J_2 = 307.808385, J_3 = 200$
Initial Euler parameters	$e_0 = 1, e_1 = e_2 = e_3 = 0$
Initial momenta ( $kg\ m^2\ rad/s$ )	$h_1 = 346.4101616, h_2 = 0, h_3 = -200$

Table 2: Model parameters and initial conditions for the second example problem

Variable	exact solution	numerical solution
Magnitude of $h_1$ ( $kg\ m^2rad/s$ )	346.4102	346.38
Magnitude of $h_2$ ( $kg\ m^2rad/s$ )	365.447	365.44
Magnitude of $h_3$ ( $kg\ m^2rad/s$ )	200.0	199.975
Period of $h_1$ (s)	9.3393	9.35
Period of $h_2$ (s)	18.6786	18.68
Period of $h_2$ (s)	18.6786	18.68
Minimum of $h_1$ ( $kg\ m^2rad/s$ )	162.6296	162.6342

Table 3: Exact versus numerical results for the second example problem

Parameter	value
Weight ( $kg\ m/s^2$ )	$W = 20$
Mass moment of inertia ( $kg\ m^2$ )	$J_1 = 5, J_2 = 5, J_3 = 1$
Initial Euler parameters	$e_0 = \cos(0.15), e_1 = \sin(0.15), e_3 = 0, e_4 = 0$
Initial angular momenta ( $kg\ m^2 rad/s$ )	$h_1 = 0, h_2 = 0, h_3 = 50$

Table 4: Simulation parameters and initial conditions for the third example problem

Variable	analytical approximation	numerical simulation
Nutation frequency ( $rad/s$ )	10.00	9.24
Precession frequency ( $rad/s$ )	0.40	0.4136

Table 5: Approximate analytical versus numerical results for the third example problem

## LIST OF FIGURES

Figure 1. First example problem, rotating disk with a translational spring suspension

Figure 2. First example problem, comparison of Euler angle based and Hamiltonian solutions for the angular momenta versus time; the computed Hamiltonian component  $h_z$  agrees with the Euler angle solution (diamond symbols) obtained using equation (46), while the Hamiltonian components  $h_x$  and  $h_y$  are identically zero

Figure 3. First example problem, numerical solution for the Euler parameters versus time; note that the Euler parameters  $e_1$  and  $e_2$  are identically zero, and along with the computed solutions for  $e_0$  and  $e_3$  determine the nonzero Euler angle in accordance with equation (2)

Figure 4. Second example problem, torque free motion of a rigid body, numerical solution for the angular momenta versus time

Figure 5. Second example problem, torque free motion of a rigid body, numerical solution for the Euler parameters versus time; note that the Euler parameters are continuous functions

Figure 6. Second example problem, torque free motion of a rigid body, computed Euler angles versus time; note the discontinuities in the Euler angles

Figure 7. Third example problem, translation and rotation of a spinning top, numerical solution for the normalized components of the angular momentum versus time

Figure 8. Third example problem, translation and rotation of a spinning top, numerical solution for the center of mass position versus time

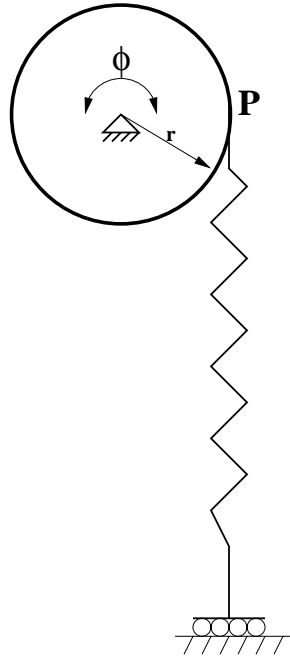


Figure 1: First example problem, rotating disk with a translational spring suspension

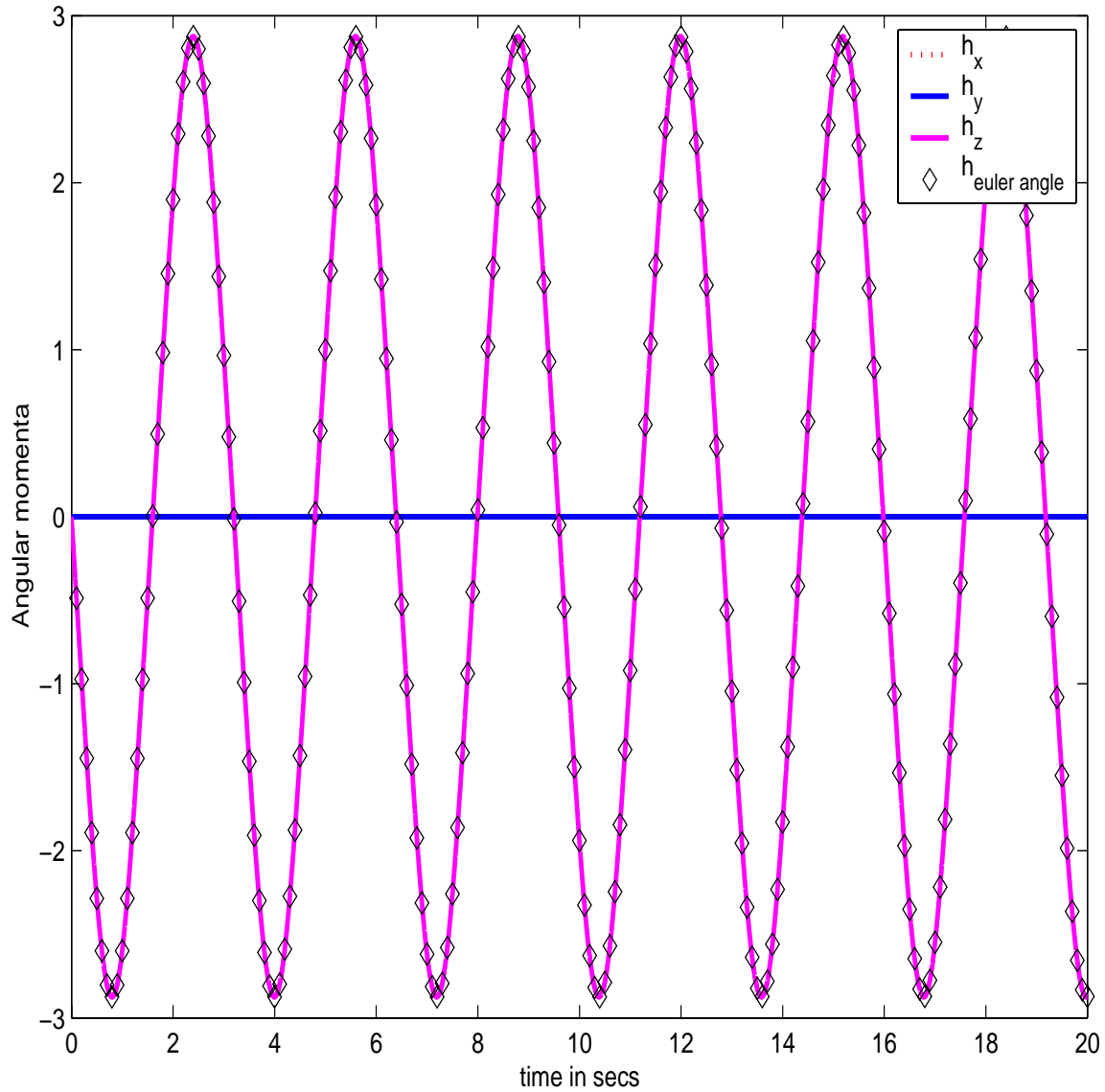


Figure 2: First example problem, comparison of Euler angle based and Hamiltonian solutions for the angular momenta versus time; the computed Hamiltonian component  $h_z$  agrees with the Euler angle solution (diamond symbols) obtained using equation (46), while the Hamiltonian components  $h_x$  and  $h_y$  are identically zero



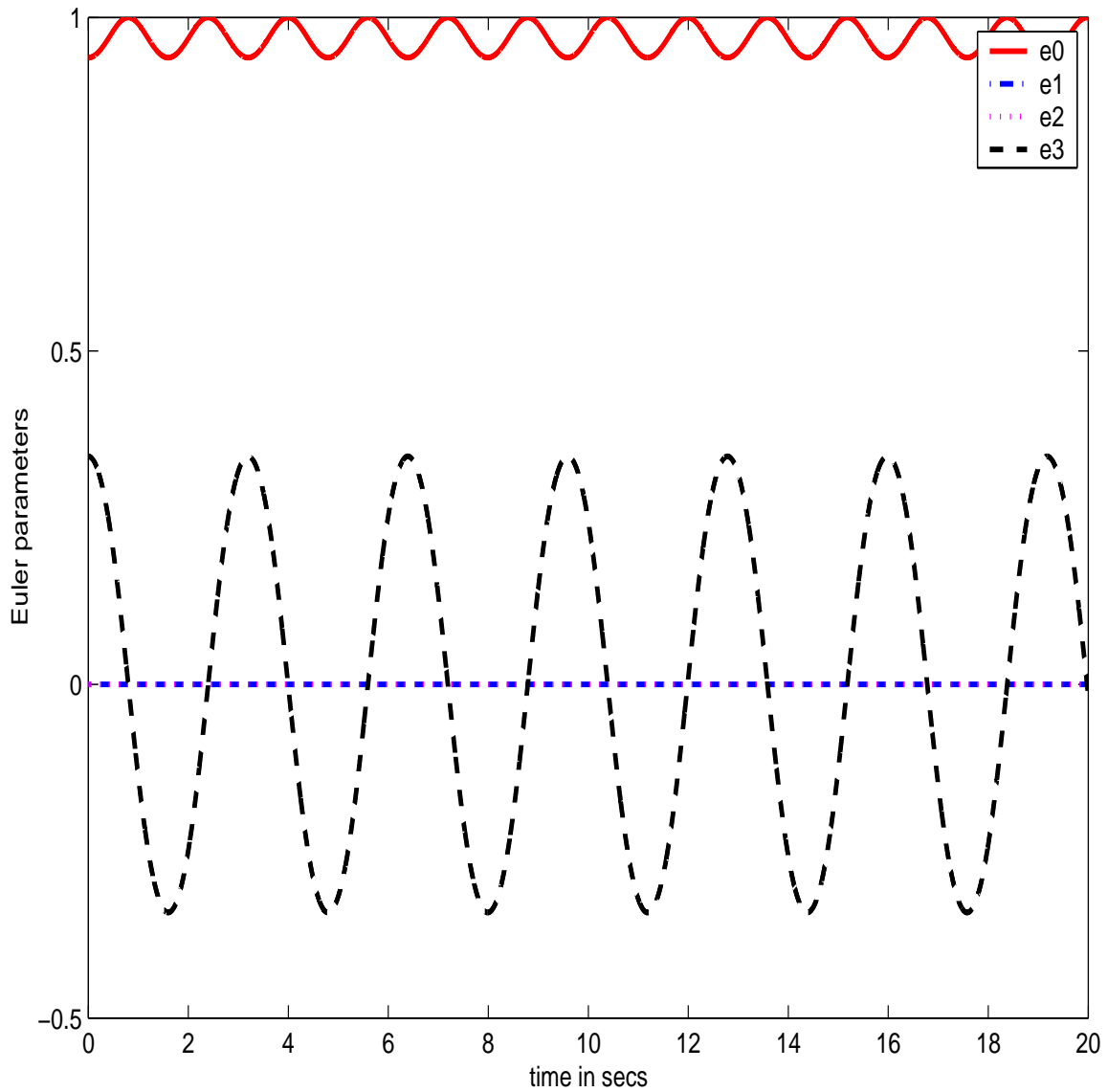


Figure 3: First example problem, numerical solution for the Euler parameters versus time; note that the Euler parameters  $e_1$  and  $e_2$  are identically zero, and along with the computed solutions for  $e_0$  and  $e_3$  determine the nonzero Euler angle in accordance with equation (2)

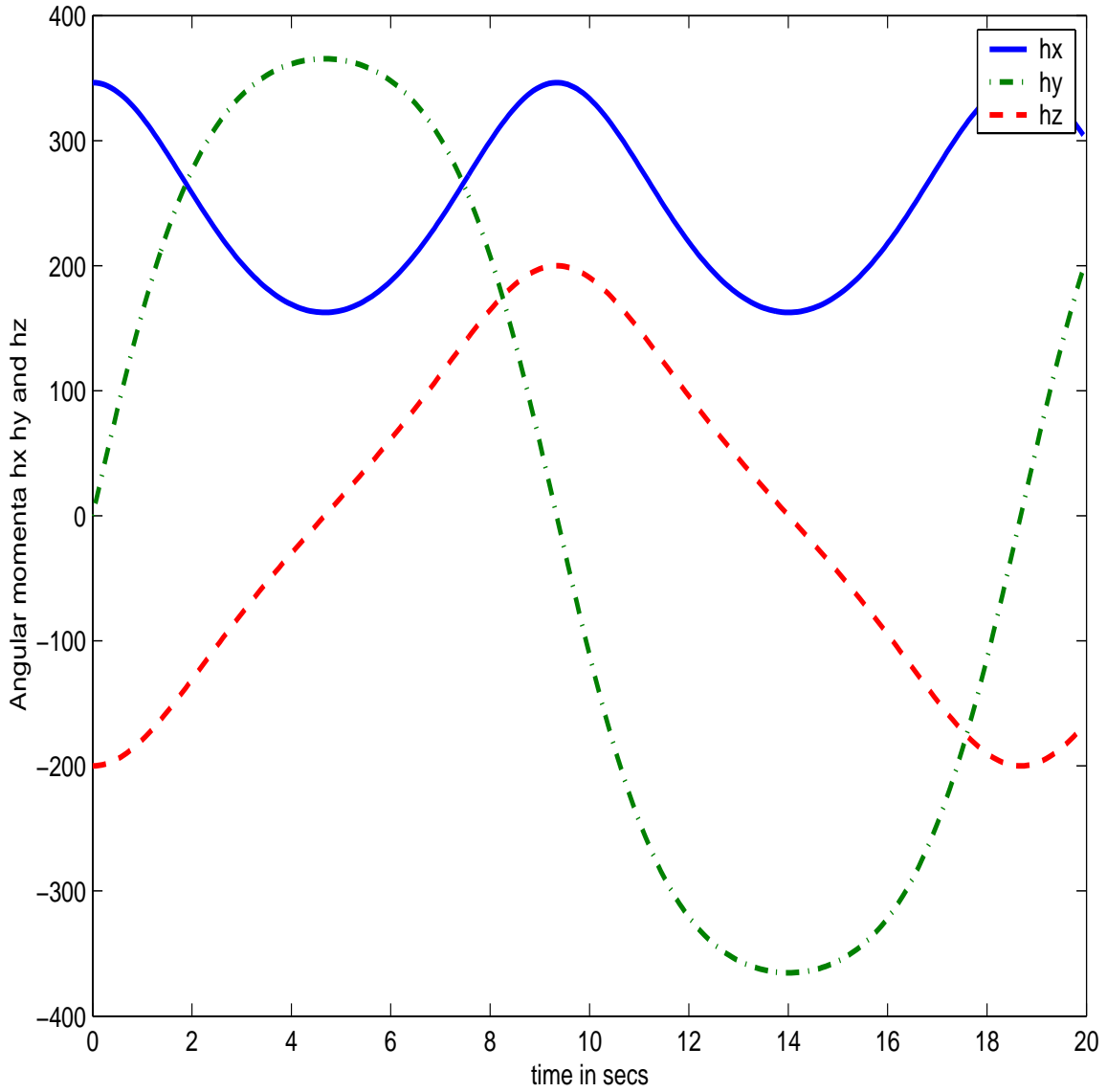


Figure 4: Second example problem, torque free motion of a rigid body, numerical solution for the angular momenta versus time

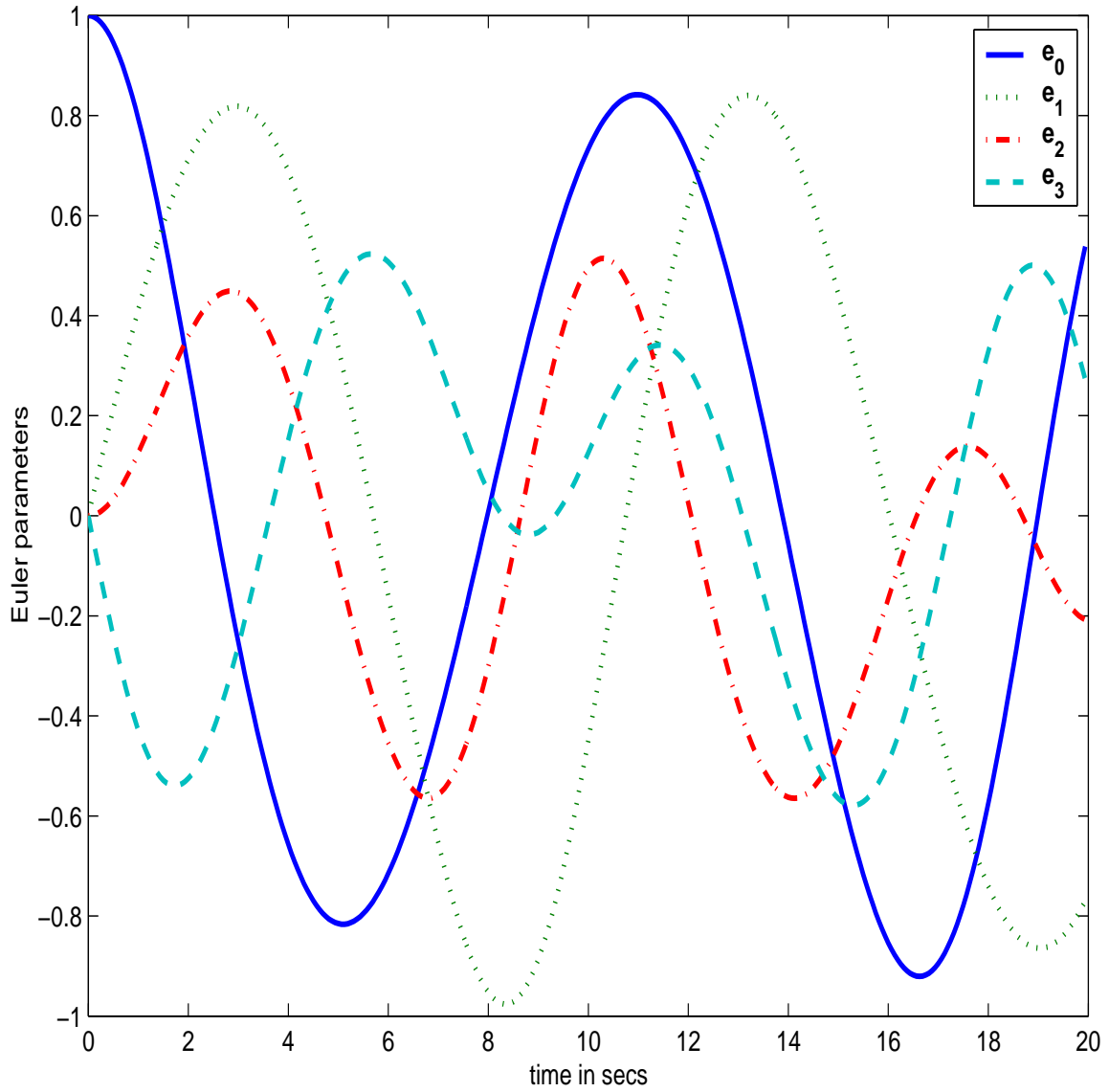


Figure 5: Second example problem, torque free motion of a rigid body, numerical solution for the Euler parameters versus time; note that the Euler parameters are continuous functions

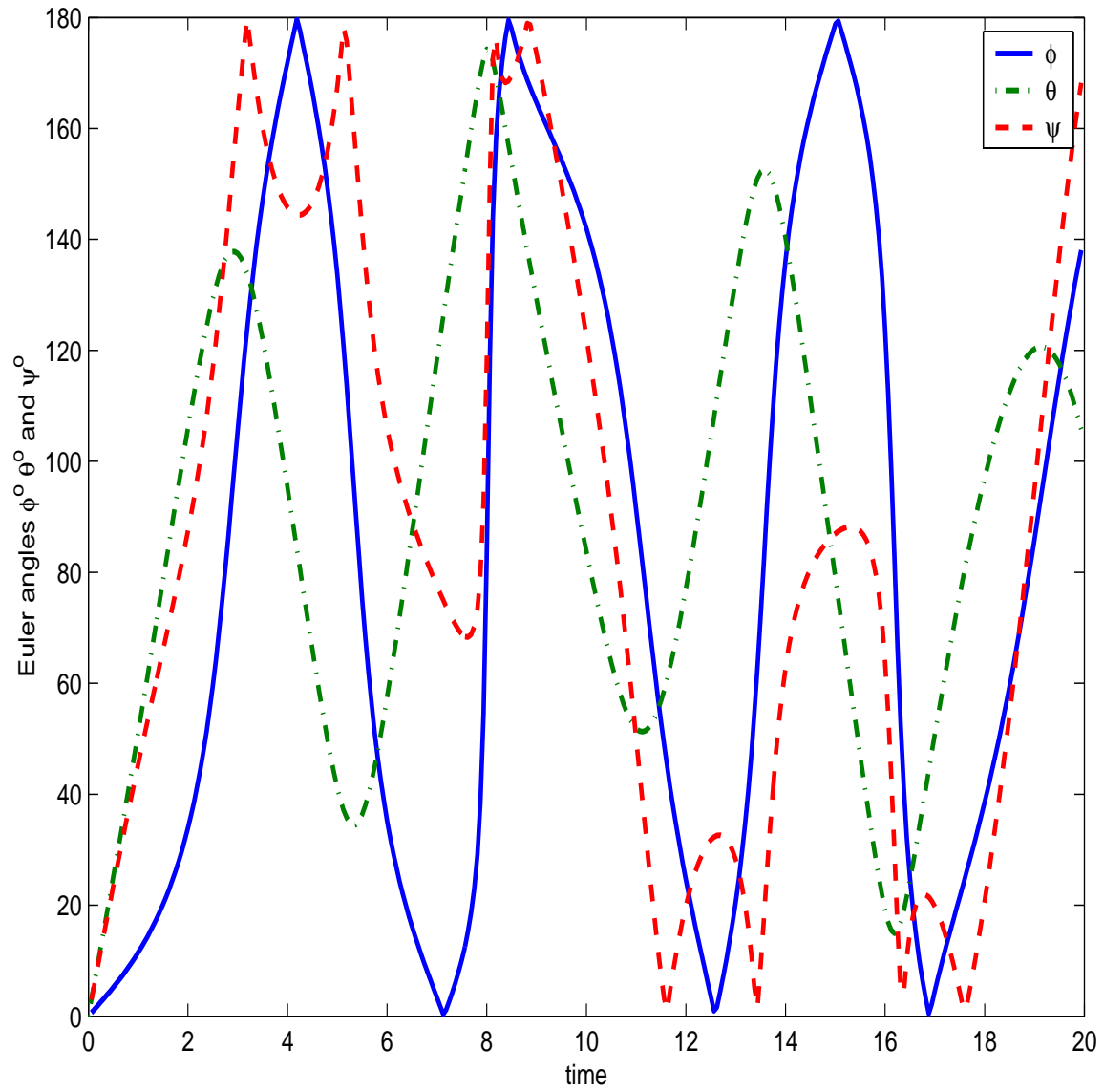


Figure 6: Second example problem, torque free motion of a rigid body, computed Euler angles versus time; note the discontinuities in the Euler angles

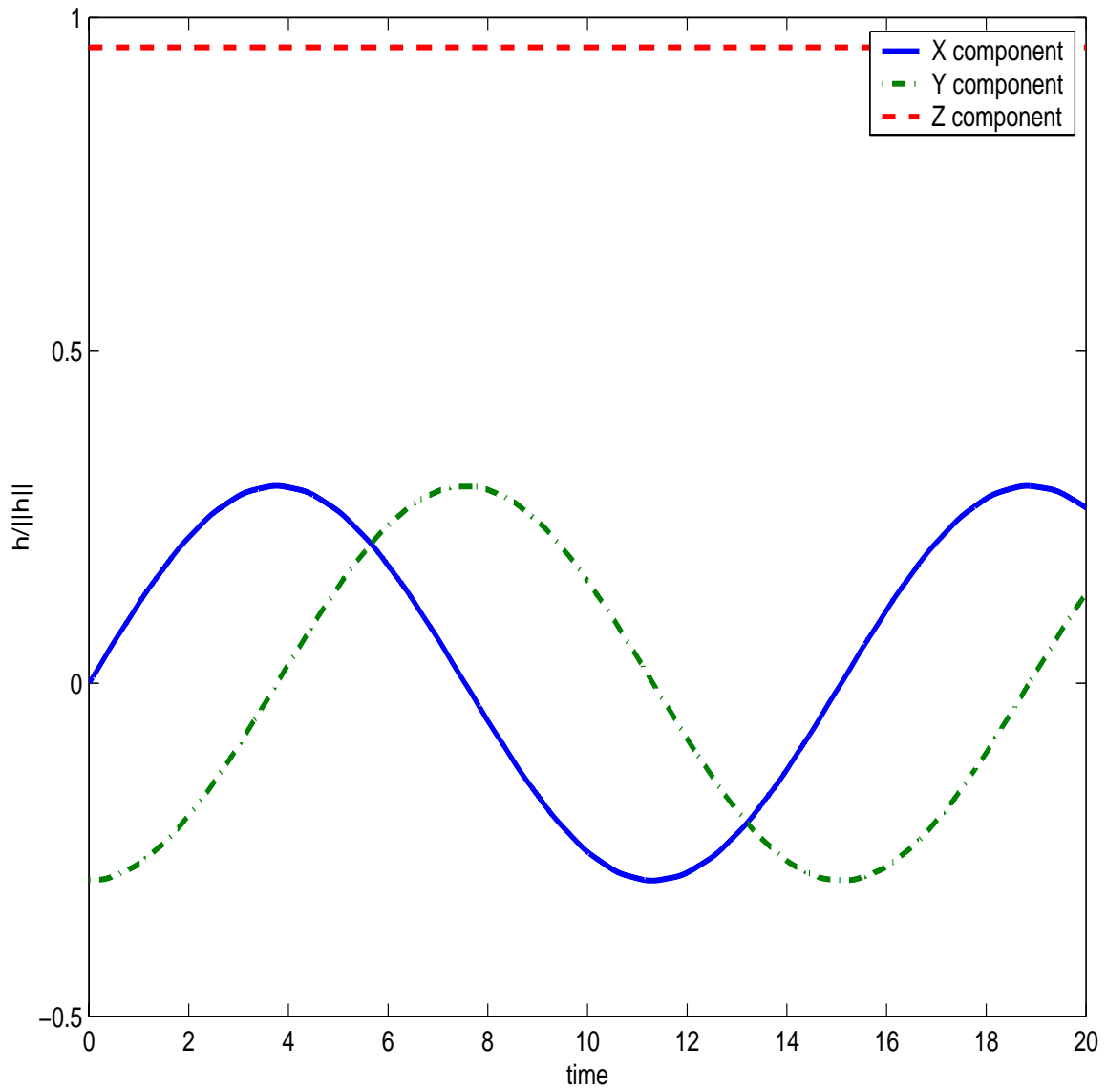


Figure 7: Third example problem, translation and rotation of a spinning top, numerical solution for the normalized components of the angular momentum versus time

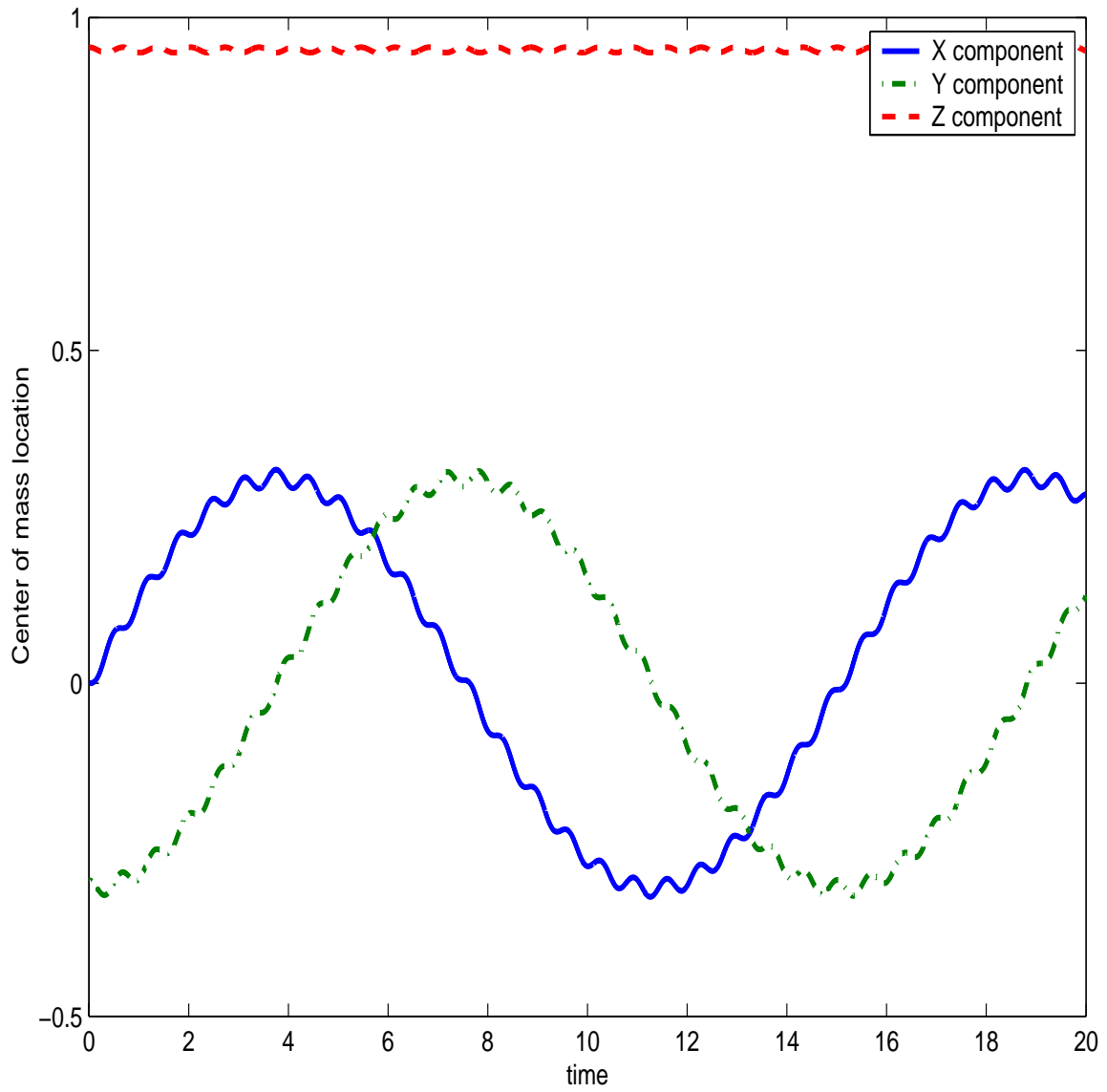


Figure 8: Third example problem, translation and rotation of a spinning top, numerical solution for the center of mass position versus time